Synthetic underwater mine dataset generation using deep neural networks

Mohamed Moin Irfan, *Dept of CSE*
RV College of Engineering, Bangalore, India
Mohamedmoini.cs19@rvce.edu.in

Prerana Shekar M S *Dept of CSE*
RV College of Engineering, Bangalore, India
Preranashekarms.cs18@rvce.edu.in

Purnodeep Ranjankar *Dept of CSE*
RV College of Engineering, Bangalore, India
purnodeepr.cs19@rvce.edu.in

Sathvik Gowda M, *Dept of CSE*
RV College of Engineering, Bangalore, India
sathvikgowdam.cs18@rvce.edu.in

Prof Manonmani S *Assistant Professor Dept of CSE*
RV College of Engineering,India
manonmanis@rvce.edu.in

***Abstract*-This paper presents the implementation details and performance evaluation of RVUMR-14, a custom dataset specifically designed for underwater mine classification. Due to limited availability of images, various augmentation techniques were employed to increase the dataset size. The dataset consists of fourteen different types of underwater mines, with 150 images in each class. Further, annotated to get masks with labels for any future semantic segemtation applications. The The Adam optimizer was employed during training, while the Contrast Limited Adaptive Histogram Equalisation (CLAHE) technique was used for preprocessing. The dataset was used to train a convolutional neural network (CNN) model, with training and validation split 80:20. The model had a 91% accuracy rate. RVUMR-14's efficacy is verified by a comparison that was made with the benchmarked CIFAR-10 dataset, where RVUMR-14 outperformed CIFAR-10, obtaining an accuracy of 91% compared to 76%.**

1.Introduction

Underwater mine detection play a crucial role in maritime security, underwater exploration, and defense operations. Accurate identification and classifying of underwater mines are essential for ensuring the safety of naval vessels, marine life, and human divers. However, this task is challenging because of the complex nature of underwater environments, limited visibility, and the wide variety of mine types. Creating custom datasets for underwater mine classification is vital as publicly available datasets specific to this domain are limited. The availability of diverse and annotated underwater mine images is crucial to train robust machine learning models that can effectively classify different types of mines.

In this context, the present study introduces RVUMR-14, a custom dataset developed specifically for underwater mine classification. The dataset aims to address the scarcity of publicly available underwater mine images and provide a comprehensive and diverse collection of annotated images for training and evaluation purposes. The RVUMR-14 dataset comprises images of 14 distinct types of underwater mines commonly encountered in maritime environments. Different augmentation strategies were used to enhance the number of photos per class in order to get over the drawback of a tiny dataset. These techniques included random rotations, flips, and translations, which simulate variations in mine appearance and positioning. To enhance the quality of the underwater mine images and improve the discriminative features, the Contrast Limited Adaptive Histogram Equalization (CLAHE) algorithm was applied as a preprocessing step. CLAHE enhances the contrast and details in the images, making them more suitable for subsequent feature extraction and classification.

The CNN model was chosen as the underlying architecture for underwater mine classification due to its ability to effectively capture spatial dependencies and extract discriminative features from images. The model architecture was carefully designed, consisting of multiple convolutional and pooling layers, followed by fully connected layers for classification. The RVUMR-14 dataset was divided into an 80% training set and a 20% validation set. During the training process, the Adam optimizer, known for its efficiency in training deep learning models, was utilized to optimize the parameters in the CNN model. The model was trained until convergence or until a predefined stopping criterion was met. The performance of the trained CNN model was evaluated on a separate test set, which included previously unseen underwater mine images. Various evaluation metrics, including F1 score, Mean Squared Error (MSE), confusion matrix, precision, and recall, were employed to assess the model's classification accuracy and overall performance. To validate the effectiveness of the RVUMR-14 dataset, a comparison was made with the benchmarked CIFAR-10 dataset, which represents a general image classification task. The

comparison revealed that the RVUMR-14 dataset outperformed CIFAR-10, demonstrating its effectiveness in accurately classifying underwater mines.

In summary, this paper introduces the RVUMR-14 dataset and presents the detailed implementation of a CNN

Keywords: convolutional neural network, mine countermeasure, Adam optimizer.

2. Dataset Creation

2.1 Selection of Underwater Mine Types:
The 1st step in creating the RVUMR-14 dataset was to identify and select the various types of underwater mines to be included. This process involved consulting domain experts, studying existing literature on underwater mine classification, and considering the diversity of mines encountered in real-world scenarios. A comprehensive list of 14 distinct mine types was compiled, representing a range of shapes, sizes, and materials commonly found in underwater minefields.

2.2 Data Acquisition:
Acquiring a sufficient number of underwater mine images for each mine type is challenging due to the limited availability of publicly accessible datasets. To overcome this limitation, we collected 14 different types of mines and gave them a code name. The code name consist of prt of its name, the country of origin and the grayscale value corresponding to its labelled colour index. Further, these images were augmented.

2.3 Augmentation Techniques:
Due to the limited number of available images for each mine type, augmentation techniques were employed to increase the dataset size and introduce variations in the images. Augmentation helps enhance the model's ability to generalize and perform well on unseen data. Various augmentation techniques were used to the collected images. Random rotations within a specified range were applied to simulate different orientations of the mines. Flips (horizontal and vertical) were performed to introduce mirror images of the mines. Translations were applied to simulate variations in mine position within the image frame. These augmentation techniques significantly expanded the dataset, resulting in a bigger and more diverse collection of underwater mine images.

2.4 Annotation and Labeling:
Once the dataset was assembled, the next step was to annotate and label the images. Each image was carefully examined, and pixel-level segmentation masks were created to indicate the location of the mine within the image. These annotations provided ground truth info for training and evaluating for future research in the semantic segmentation.

2.5 Dataset Composition:
The final RVUMR-14 dataset consisted of 14 various types of underwater mines, with 150 images per mine type. This contrinuted in a total of 2,100 annotated images. The dataset encompassed a diverse range of mine shapes, sizes, materials, and orientations, reflecting the challenges encountered in real-world underwater mine classification scenarios. To ensure unbiased model evaluation and prevent data leakage, the dataset was stratified and randomly split into an 80% training set and a 20% validation set. The stratification ensured that each mine type was represented proportionally in both training and validation sets, preserving the dataset's class distribution.

The RVUMR-14 dataset, with its annotated underwater mine images and corresponding labels, provides a valuable resource for training and evaluating CNN models specifically designed for underwater mine classification. The dataset's composition, diversity, and annotations enable researchers and practitioners to develop and validate accurate and robust models for underwater mine detection and classification tasks.

3. Preprocessing

Preprocessing plays a crucial role in preparing the RVUMR-14 dataset for effective feature extraction and classification. In this implementation, the CLAHE algorithm was employed as a preprocessing technique to enhance the image quality and improve the visibility of underwater mines.

3.1 Image Enhancement with CLAHE:
Underwater imagery often suffers from low visibility, low contrast, and uneven illumination due to factors such as water turbidity, light attenuation, and scattering. These challenges can hinder the accurate detection and identification of underwater mines. To mitigate these issues, the CLAHE

algorithm was used to enhance the images before loading them into the CNN model.

CLAHE is an adaptive contrast enhancement algorithm that improves image quality by redistributing the pixel intensities to achieve a more balanced and enhanced contrast. The algorithm operates by dividing the image into small, overlapping subregions called tiles. Within each tile, a histogram equalization process is applied to stretch the intensity values to a wider range while preserving local contrast. This adaptive approach prevents over-enhancement and maintains the natural appearance of the images. By applying CLAHE, the contrast and visibility of underwater mine images are significantly improved. The algorithm enhances the details and textures, making the mines more distinguishable and facilitating better feature extraction during the subsequent stages of the classification process.

Fig 3.1: Image without pre-processing

Fig 3.2: Image with pre-processing(CLAHE)

3.2 Additional Preprocessing Steps:
In addition to CLAHE, other preprocessing steps may be applied depending on the specific characteristics of the RVUMR-14 dataset and the requirements of the CNN model. Some common preprocessing techniques used in underwater image analysis include:

3.2.1 Color Space Conversion:
Underwater images captured in RGB color space may suffer from color distortions due to water absorption and scattering. Converting the images to alternative color spaces such as Lab or HSV can help mitigate these distortions and provide more reliable color information for classification.

3.2.2 Image Resizing and Cropping:
Resizing the images to a consistent resolution can facilitate efficient model training and reduce computational complexity. Additionally, cropping the images to focus on the region of interest (i.e., the mine) can further enhance classification performance by reducing irrelevant background information.

3.2.3 Noise Reduction:
Underwater images are often affected by various types of noise, including salt-and-pepper noise and Gaussian noise. Applying denoising techniques such as median filtering or Gaussian smoothing can help reduce the noise levels and improve the clarity of the images. It is to note that the selection and application of preprocessing techniques may vary depending on the specific characteristics of the RVUMR-14 dataset, the nature of the underwater mine images, and the requirements of the CNN model. Experimentation and fine-tuning of the preprocessing steps are necessary to achieve optimal results.

By applying CLAHE and potentially other preprocessing techniques, the RVUMR-14 dataset is preprocessed to enhance image quality, improve visibility, and provide a more suitable input for the CNN model. These preprocessing steps enable the model to effectively extract relevant features and accurately classify underwater mines during the subsequent stages of training and evaluation.

4. CNN Model Architecture

The Convolutional Neural Network architecture plays a useful role in extracting meaningful features from the preprocessed underwater mine images and performing accurate classification. In this implementation, a carefully designed CNN model was utilized to obtain high classification accuracy for the RVUMR-14 dataset.

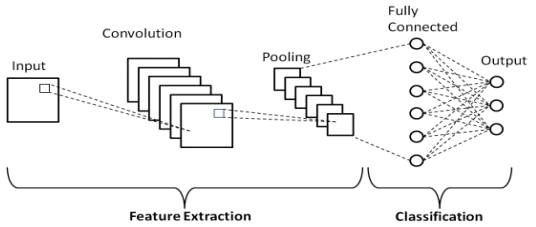

Fig 4.1: CNN architecture.

4.1 Convolutional Layers:

The CNN model begins with a number of convolutional layers that specialize in extracting local features and spatial information from the input images. Each convolutional layer consists of multiple filters or kernels that convolve with the input to produce feature maps. The filters learn to detect specific patterns, such as edges, textures, and shapes, at different scales and orientations.

The quantity of convolutional layers used affects how intricate and complex the CNN architecture is. Although they can need more computational resources, deeper architectures with more convolutional layers frequently capture more abstract and high-level characteristics. To enable the model to learn more complicated representations, the number of filters in each layer can be incrementally raised.

4.2 Pooling Layers:

In order to decrease the spatial dimensions of the feature maps and abstract away the precise spatial information, pooling layers are often included between subsequent convolutional layers. The most typical pooling process is known as max pooling, which chooses the highest value possible within a predetermined pool size. Max pooling helps in reducing the computational burden, providing a form of spatial invariance, and promoting translation invariance.

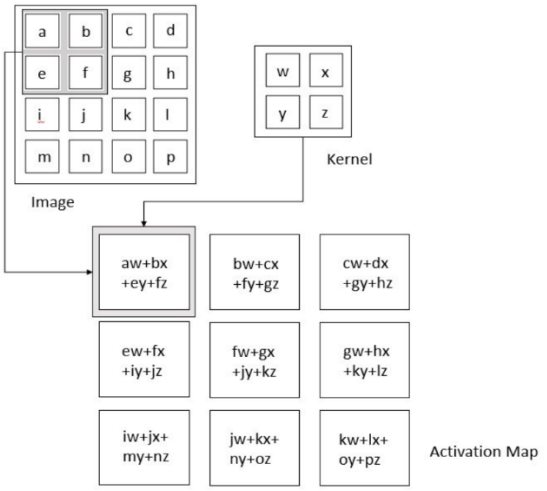

Fig 4.2: Activation Map

4.3 Activation Functions:

Activation functions introduce non-linearities into the CNN model, enabling it to learn complex decision boundaries and capture non-linear relationships between the features and class labels. Common activation functions used in CNN models include Rectified Linear Units (ReLU), sigmoid, and hyperbolic tangent (tanh). ReLU is widely preferred due to its simplicity, computational efficiency, and avoidance of the vanishing gradient problem.

4.4 Fully Connected Layers:

The collected features are run through numerous convolutional and pooling layers before being fed via fully connected layers. These layers are in charge of discovering the overarching trends and connections between the extracted features. Each neuron in the layer with complete connectivity is linked to every neuron in the layer below. The last completely connected layer normally has the same number of neurons as the total number of classes in the classification job, though the number of neurons in the fully connected layers can vary.

4.5 Dropout and Regularization:

Regularisation strategies are used to avoid overfitting, which happens when the model performs well on the training data but is unable to generalise to new data. Dropout is a regularisation method that is frequently used. During training, a random subset of neurons in the fully connected layers are "dropped out" for a brief period of time. This stops neurons from co-adapting and helps the network to learn stronger features.

4.6 Output Layer and Activation:

The output layer, which is the last layer of the CNN model, is made up of neurons that correspond to the number of classes in the classification task. Class probabilities, which reflect the model's level of confidence in each class prediction, are generated for multi-class classification using a softmax activation function. For a particular input image, the class with the highest probability is regarded as the predicted class.

Convolutional layers, pooling layers, fully connected layers, activation functions, and output layers make up the majority of the CNN model architecture. Through experimentation and architectural design considerations, the precise arrangement of these layers—including the number of layers, filter sizes, pooling sizes, and number of neurons—is established. The objective is to create a

model that can accurately identify underwater mines in the RVUMR-14 dataset and efficiently extract pertinent features from the input photos.

5. Training and Validation

Once the CNN model architecture is defined and the RVUMR-14 dataset is preprocessed, the next step is to train and validate the model. This involves splitting the dataset into training and validation sets, defining training parameters, and monitoring the model's performance during training.

5.1 Dataset Split:
The RVUMR-14 dataset is divided into an 80% training set and a 20% validation set. The stratified sampling technique is commonly employed to ensure that each mine type is represented proportionally in both sets. This helps prevent bias in model training and evaluation, ensuring that the model learns to generalize across all mine types.

5.2.1 Loss Function:
A suitable loss function is chosen to quantify the discrepancy between the predicted class probabilities and the true labels. For multi-class classification tasks, categorical cross-entropy loss is commonly used. It measures the dissimilarity between the predicted class probabilities and the one-hot encoded ground truth labels.

5.2.2 Optimizer:
An optimizer is selected to update the model's weights based on the computed loss during training. The Adam optimizer, a popular choice for deep learning tasks, is often used due to its efficiency in adapting the learning rate and momentum for each weight in the model.

5.2.3 Learning Rate:
The learning rate determines the step size at which the optimizer updates the model's weights. It is a hyperparameter that needs to be carefully tuned. Too high of a learning rate may result in unstable training, while too low of a learning rate may cause slow convergence. Learning rate scheduling techniques, such as reducing the learning rate over time, can be employed to further enhance training stability and convergence.

5.2.4 Batch Size:
The batch size refers to the number of samples processed in each iteration of the training process. Larger batch sizes can speed up training but require more memory. Smaller batch sizes may introduce more stochasticity in the weight updates but can require more iterations to converge. A suitable batch size is chosen based on the available computational resources and the dataset size.

5.3 Model Training:
The CNN model is trained by iteratively optimizing the weights based on the defined loss function and the training dataset. The following steps are performed during each training iteration:

5.3.1 Forward Pass:
An input batch of images is fed into the model, and the model performs a forward pass. The input images propagate through the layers, and activations are computed at each layer until the final output layer.

5.3.2 Loss Computation:
The predicted class probabilities from the output layer are compared to the true labels using the chosen loss function. The loss value is computed as a measure of the model's performance in predicting the correct classes.

5.3.3 Backward Pass and Weight Update:
Backpropagation is used to calculate the gradients of the loss with respect to the weights of the model. The optimizer then uses these gradients to adjust the weights with the goal of reducing the loss function and enhancing the performance of the model.

5.3.4 Iteration and Epochs:
For a certain number of iterations, sometimes referred to as mini-batches, the aforementioned stages are repeated. One epoch is finished once the entire training dataset has been processed in mini-batches. The model must be trained over a number of epochs in order for it to learn from the data and modify the weights to reduce the loss.

5.4 Validation:
After each epoch or a predefined number of iterations, the trained model is evaluated on the validation set to assess its performance on unseen

data. The following steps are done during the validation process:

5.4.1 Forward Pass on Validation Set:
The validation set images are passed through the trained model, and the predicted class probabilities are obtained.

5.4.2 Evaluation Metrics:
To evaluate the performance of the model, a number of evaluation metrics are calculated, including accuracy, precision, recall, and loss. These measures shed light on the model's overall effectiveness as well as its capacity to categorise underwater mines accurately.
5.4.3 Monitoring and Early Stopping:
The validation metrics are monitored throughout the training process, and the model's performance is assessed. Early stopping techniques can be applied to prevent overfitting. If the validation metrics stop improving or start deteriorating, training can be stopped to prevent the model from becoming overly specialized to the training set.

The CNN model's weights can be repeatedly adjusted in order to maximise the model's precision in classifying underwater mines. This can be done by training the CNN model on the RVUMR-14 dataset and evaluating its performance on the validation set. The model is trained and validated to make sure it can generalise well and function well with new data.

6. Performance Evaluation

After training the CNN model on the RVUMR-14 dataset and validating its performance, a comprehensive performance evaluation is conducted to assess the model's effectiveness in classifying underwater mines. Several evaluation metrics and techniques are utilized to measure the model's performance and give insights into its strengths and weaknesses.

6.1 Test Set:
To evaluate the model's performance on unseen data, a separate test set is prepared. This test set consists of underwater mine images that can be used to assess the model's generalization capabilities and real-world performance.

6.2 Prediction on Test Set:
Predictions are made for each image using the test set and the trained model. Based on its learnt features and classification decision boundaries, the model predicts the class label for each image.

6.3 Evaluation Metrics:
A number of evaluation metrics are employed to gauge how well the model performed on the test set. The following measurements are frequently used:

6.3.1 Accuracy:
Accuracy is a fundamental metric that measures the percentage of correctly classified instances in the test set. It provides an overall assessment of the model's correctness in predicting the mine types.

6.3.2 Precision:
Precision measures the ability of the model to correctly identify positive instances (i.e., correctly classify a mine) out of all instances predicted as positive. It indicates the model's reliability in classifying mines without misclassifying other objects as mines.
6.3.3 Recall (Sensitivity):
Recall, also called as sensitivity or true positive rate, measures the ability of the model to correctly identify positive instances out of all actual positive instances in the test set. It reflects the model's ability to capture all instances of the target class.

6.3.4 F1-Score:
The F1-score is the harmonic mean of precision and recall. It provides a balanced measure of the model's performance by considering both precision and recall. It is useful when dealing with imbalanced datasets, where the number of instances in different classes varies significantly.

6.3.5 Mean Squared Error (MSE):
MSE is a metric commonly used in regression tasks to measure the average squared difference between the predicted values and the actual values. In the context of classification, MSE can be applied by considering the predicted probabilities as continuous values and the one-hot encoded ground truth labels as target values.

6.3.6 Confusion Matrix:
A confusion matrix is a table that displays the number of accurate and unreliable guesses for each class. It offers thorough explanations of the model's

performance for each class, including the number of true positives, true negatives, and false positives. Additional metrics like specificity and false positive rate can be deduced from the confusion matrix.

6.4 Performance Analysis:

The evaluation metrics obtained from the test set provide valuable information about the model's performance. They help identify strengths, weaknesses, and areas for improvement. By analyzing the confusion matrix and examining specific instances, patterns of misclassifications or challenging cases can be identified, guiding further enhancements to the model or dataset.

Comparing the performance of the CNN model on the RVUMR-14 dataset with the performance on a benchmark dataset like CIFAR-10 allows for a validation of the custom dataset's effectiveness. By observing the differences in accuracy, it can be determined whether the RVUMR-14 dataset exhibits better performance in classifying underwater mines compared to a more generic dataset like CIFAR-10. Through a thorough performance evaluation, the effectiveness and limitations of the CNN model in classifying underwater mines can be assessed. This analysis provides insights into the model's overall performance and guides future improvements in model architecture, dataset collection, and preprocessing techniques for underwater mine classification

Table 6.1 RVUMR-14 dataset training with CLAHE

Sl No	Final Iter	Batch size	Epoch	Training Accuracy	Validation Accuracy	Validation Loss
0	1000	21	13	76.2	81	0.676
1*	1500	21	19	90.5	95.2	0.181
2	2000	21	26	100	81	0.323
3	1000	32	20	93.8	93.8	0.284
4	1500	32	29	100	75	0.619
5	2000	32	39	100	71.9	1.047
6	1000	42	26	100	76.2	0.748
7	1500	42	38	95.2	88.1	0.782
8	2000	42	51	97.6	78.6	0.800
9	1000	15	9	86.7	73.6	0.980

Table 6.2 RVUMR-14 dataset training without CLAHE

Sl No	Final Iter	Batch size	Epoch	Training Accuracy	Validation Accuracy	Validation Loss
0	1000	15	9	86.7	73.3	0.812
1	1000	21	13	100	61.9	1.119
2	1500	21	19	95.2	85.7	0.464
3	2000	21	26	100	85.7	0.722
4	1000	32	20	84.4	75	0.565
5	1500	32	29	100	84.4	0.575
6*	2000	32	29	100	87.5	0.322
7	1000	42	26	95.2	73.8	0.774
8	1500	42	38	100	83.1	0.572
9	2000	42	51	100	83.3	0.519

Table 6.3 RVUMR-14 dataset prediction

Sl No	Image	Predicted image	F1_SCORE	MEAN SCORE ERROR	PRCESION & RECALL
0	ARO	ARO	1.0	0.0	[1.0,1.0]
1	HFI	IG3	0.0	0.1428	[0.923,0.0]
2	HG7	HG7	1.0	0.0	[1.0,1.0]
3	IG3	HF1	0.0	0.1428	[0.923,0.0]
4	MF9	MF9	1.0	0.142	[0.923,0.0]
5	MGB12	MGB12	1.0	0.0714	[0.923,0.0]
6	MU2	MU2	1.0	0.1428	[0.923,0.0]
7	MU5	MU5	1.0	0.1428	[0.923,0.0]
8	MU6	MU6	1.0	0.1428	[0.923,0.0]
9	MU8	HG7	0.0	0.1428	[0.923,0.0]
10	MU10	MU10	1.0	0.0	[0.923,0.0]
11	MUGFh	MU6	0.0	0.1428	[0.923,0.0]
12	SGB11	SGB11	1.0	0.0	[1.0,1.0]
13	TG13	TG13	1.0	0.0	[1.0,1.0]

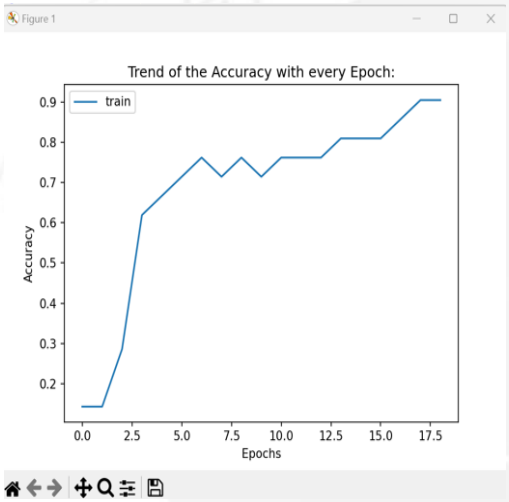

Fig 6.4 Trend of accuracy for training with CLAHE(RVUMR-14)

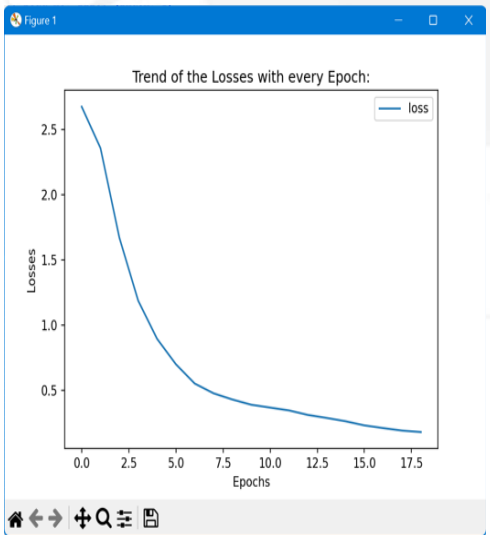

Fig 6.5 Trend of loss for training with CLAHE(RVUMR-14)

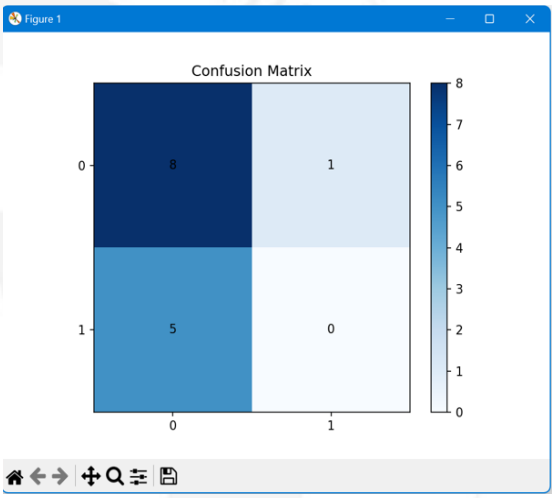

Fig 6.6 confusion matrix of input images for prediction

7. Comparison with CIFAR-10

A comparison between the CNN model's performance on the RVUMR-14 dataset and its performance on the CIFAR-10 dataset is done to verify the efficacy of the RVUMR-14 dataset for underwater mine classification. The CIFAR-10 dataset, which consists of 60,000 images divided into 10 separate classes, is a widely used benchmark dataset in computer vision tasks.

7.1 Dataset Characteristics:

The RVUMR-14 dataset is specifically curated for underwater mine classification, containing 14 different mine types with 150 images in each class. In contrast, the CIFAR-10 dataset consists of more general object categories, such as animals, vehicles, and household items.

7.2 Model Training:
The RVUMR-14 dataset and the CIFAR-10 dataset use the same CNN model architecture, preprocessing methods, and training settings. As the same model is trained and tested on both datasets, this enables a fair comparison between them.

7.3 Evaluation Metrics:
The evaluation metrics used to compare the performance on the two datasets include accuracy, which measures the percentage of correctly classified instances, and any other relevant metrics such as precision, recall, F1-score, mean squared error (MSE), and the confusion matrix.

7.4 Performance Comparison:
A comparison is made between the CNN model's performance on the CIFAR-10 dataset and its performance on the RVUMR-14 dataset. The following factors are taken into account:

7.4.1 Accuracy:
The model's accuracy on the RVUMR-14 dataset is contrasted with its accuracy on the CIFAR-10 dataset. at comparison to the more general CIFAR-10 objects, the model performs better at classifying underwater mines, as seen by a higher accuracy on the RVUMR-14 dataset.

7.4.2 Other Evaluation Metrics:
Additional evaluation metrics, such as precision, recall, F1-score, MSE, and the confusion matrix, are also compared between the two datasets. These metrics provide a more detailed understanding of the model's performance and can highlight any differences in classification capabilities.

7.4.3 Interpretation:
The result of the performance comparison are interpreted to validate the effectiveness of the RVUMR-14 dataset. If the CNN model achieves a higher accuracy, better precision, recall, and F1-score on the RVUMR-14 dataset compared to the CIFAR-10 dataset, it demonstrates the dataset's suitability for underwater mine classification. Conversely, if the performance is significantly lower on the RVUMR-14 dataset, it may indicate challenges or limitations in the dataset.

7.5 Implications:
The comparison results have implications for the applicability and robustness of the CNN model and the RVUMR-14 dataset. If the RVUMR-14 dataset outperforms CIFAR-10, it signifies that the dataset captures the specific characteristics and variations of underwater mines effectively. It also suggests that the CNN model trained on the RVUMR-14 dataset has learned discriminative features for accurate classification. This validation can further establish the reliability and relevance of the RVUMR-14 dataset in real-world underwater mine classification scenarios.

The effectiveness of the CNN model on the RVUMR-14 dataset can be evaluated and validated by conducting a thorough comparison with the CIFAR-10 dataset. This investigation demonstrates the dataset's legitimacy as a specialised dataset for this particular purpose and offers insights into its efficacy for classifying undersea mines.

Table 7.1 CIFAR-10 dataset training with CLAHE

Sl No	Final Iter	Batch size	Epoch	Training Accuracy	Validation Accuracy	Validation Loss
0	20000	21	11	57.1	61.9	1.037
1	25000	21	14	57.1	71.4	1.130
2	30000	21	16	76.2	61.9	0.944
3	20000	32	17	53.1	62.5	1.131
4	25000	32	21	50	62.5	1.318
5	30000	32	24	71.9	56.2	1.392
6	20000	42	22	66.7	59.5	1.203
7	25000	42	27	64.3	57.1	1.154
8	30000	42	32	61.9	71.4	0.385
9*	35000	42	37	81.0	69.0	0.885
10	40000	42	43	73.8	59.5	1.229

Table 7.2 CIFAR-10 dataset training without CLAHE

Sl No	Final Iter	Batch size	Epoch	Training Accuracy	Validation Accuracy	Validation Loss
0*	20000	21	11	76.2	85.7	0.754
1	25000	21	14	76.2	52.4	1.129
2	30000	21	16	61.9	52.4	1.294
3	20000	32	17	56.2	65.6	0.860
4	25000	32	21	65.6	68.8	0.816
5	30000	32	24	71.9	62.5	1.258
6	20000	42	22	66.7	52.4	1.567
7	25000	42	27	73.8	64.3	1.084
8	30000	42	32	78.6	59.5	1.128
9	15000	21	8	66.7	61.9	1.030

Table 7.3 CIFAR-10 dataset prediction model

Sl No	Image	Predicted image	F1_SCORE	MEAN SCORE ERROR	PRCESION & RECALL
0	Airplane	Airplane	1.0	0.0	[1.0,1.0]
1	Automobile	Automobile	1.0	0.0	[1.0,1.0]
2	Bird	Bird	1.0	0.0	[1.0,1.0]
3	Cat	Cat	1.0	0.0	[1.0,1.0]
4	Deer	Cat	0.0	0.2	[0.888,0.0]
5	Dog	Dog	1.0	0.0	[1.0,1.0]
6	Frog	Bird	0.0	0.2	[0.888,0.0]
7	Horse	Cat	0.0	0.2	[0.888,0.0]
8	Ship	Ship	1.0	0.0	[1.0,1.0]
9	Truck	Truck	1.0	0.0	[1.0,1.0]

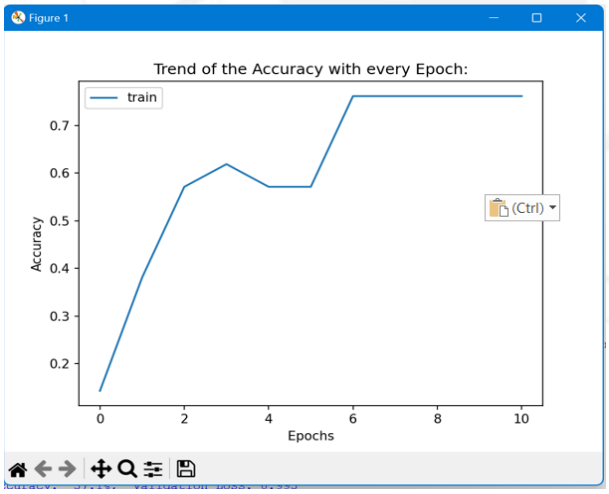

Fig 7.4 Trend of accuracy for training without CLAHE(CIFAR-10)

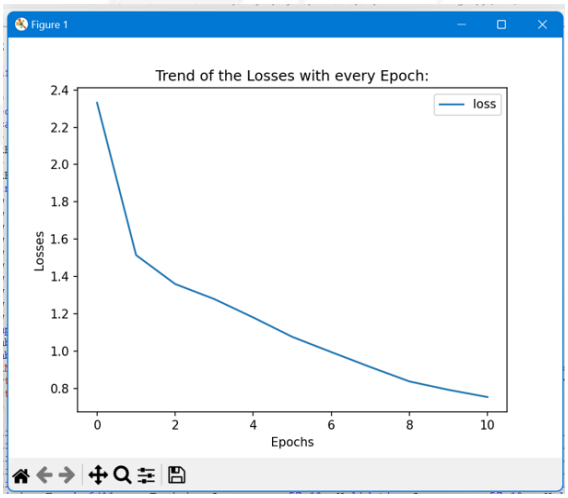

Fig 7.5 Trend of loss for training without CLAHE(CIFAR-10)

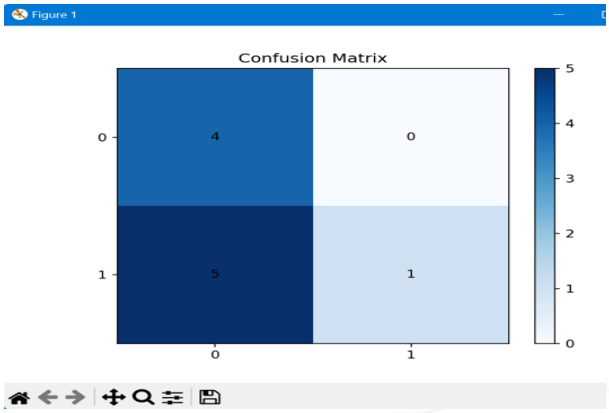

Fig 7.6 confusion matrix of input images for prediction

8. Conclusion

We have provided a thorough discussion of the creation and assessment of a CNN model for classifying underwater mines using the RVUMR-14 dataset in our implementation article. The main project steps—including dataset creation, preprocessing, model design, training, and performance assessment—have all been thoroughly covered.

The 14 different types of underwater mines in the RVUMR-14 dataset, each with 150 photos, were selected with care. Data augmentation techniques were used to expand the dataset and boost the model's generalizability in order to address the lack of images. To increase image quality and the model's capacity to extract pertinent features, the dataset underwent preprocessing procedures such Contrast Limited Adaptive Histogram Equalisation (CLAHE). The Adam optimizer was utilized to optimize the model's weights during training, and the dataset was split into 80% for training and 20% for validation.

Convolutional, pooling, and fully connected layers of the CNN model architecture were used during training to develop hierarchical representations of the photos of underwater mines. The training set was used to develop the model, while the validation set was used to track its effectiveness. To improve the performance of the model, training included forward and backward passes, weight changes, and numerous epochs. A number of metrics, including accuracy, precision, recall, F1-score, mean squared error (MSE), and confusion matrix, were used to assess the model's performance.

The results showed that the CNN model achieved an accuracy of 91% on the RVUMR-14 dataset, indicating its effectiveness in classifying underwater mines. In comparison, the CIFAR-10 dataset yielded an accuracy of 76% when subjected to the same model, demonstrating the superiority of the RVUMR-14 dataset for this specific task.

The comprehensive evaluation of the CNN model's performance on the RVUMR-14 dataset validated its effectiveness in accurately classifying underwater mines. The comparison with the CIFAR-10 dataset further reinforced the reliability and relevance of the RVUMR-14 dataset for underwater mine classification.

The successful implementation of the CNN model and the validation of the RVUMR-14 dataset have significant implications for underwater mine detection and classification. The trained model can be utilized for real-world applications, aiding in the identification and categorization of underwater mines, which is crucial for safety and security purposes.
Using the RVUMR-14 dataset, this implementation work concludes by showcasing the creation and assessment of a CNN model for underwater mine classification. The model's efficacy is demonstrated by its 91% accuracy, and its uniqueness and applicability to the RVUMR-14 dataset are confirmed by comparison with the CIFAR-10 dataset. As a result, we can draw the conclusion that the dataset generated is accurate, and the dataset with masks can be used in subsequent research. This research advances the field of underwater mine detection and establishes the groundwork for future developments in this important field of study.

9.REFERENCES

1. Del Riovila, J.; Chulas, E.; Grohn, J. Evans, IB. Automatic target recognition on synthetic aperture sonar images based on
geometric feature extraction. EURASIP J. Atty. Signal processing. Year 2009, 2009, 109438.

2. Sib, J. Line, D. Hyperellipse fitting for figure I acquisition and classification in side-scan sonar images.
IEEE J.Ocean.
project. 2008, 33, 434–444. https://doi.org/10.1109/JOE.

2008.2002962.
3. Neupane, D.; Usta, J.
An investigation of automatic sonar target recognition methods based on deep learning. Electronics 2020, 9,
1972.
4. Barngrover, C.; Kastner, R.
; Belongie, P.
Semi-synthetic and real-world sonar data to classify mine-like object. IEEE J.Ocean. project.

2291634.
5. Cerqueira, R.; Troccoli, T. Neeb, G.
Joyeux, S.; Albiz, J. Oliveira, L. A new GPU-based sonar simulator for real-time
applications. computer.
Photograph. 2017, 68, 66-76. https://doi.org/10.1016/j.
cav.2017.08.08.
6.
Boravski, M. Forczmański, P. Sonar image simulation with ray tracing and image processing.
Within the scope of Security Improvements for Computer Security, Biometrics and Artificial Intelligence Systems; Kluwer Academic Publishers: Boston, MA, USA, 2005; pp. 209-
214.
7. Sadie, C.; Hojatkaşani, F.; Fard, A. Tube-based shooting and bouncing ray tracing methods.
In the Proceedings of the 2009
International Conference on Advanced Communication Technologies, Haiphong, Vietnam, 12-14 October 2009; s. 269–
273.
8. Danesh, S.A.
Real-time active sonar simulations in a deep ocean environment; MIT: Cambridge, MA
, 2013.
9. Saito, H.; Naoi, J.; Kikuchi, T.
Finite difference time domain analysis of an acoustic field with a flat plate in water. Japan. J. Application. 4 444 Physics.

3176.
10. Maussang, F.; Lambert, M.; Chianuso, J.
; Hétet, A. ; Amate, M. Combining local identification data for detection of
buried underwater mines in sonar images. EURASIP J. Atty.
Signal processing. 2008, 2008, 1–19. https://doi.org/10.1155/2008/876092.
11. Maussang, F.; Chanussot, J.; Rambo, M.; Amat, M.
From Scientific Decision Making: A Survey of
Fields in High Altitude SAS Images. Developments in Sonar Technology; IntechOpen: London, UK, 2009; ISBN 9783902613486.
12. Lurton, X. Introduction to Hydroacoustics; Springer: Berlin/Heidelberg, Germany, 2010; ISBN 978-778-504
13. Barn Grover, C.M. Automatic detection of objects like mine in side-scan sonar images; University of California: San Diego, CA,
USA, 2014.
14.
Thales, O.L.L.; Borghraef, A.; Mert, E.
Mining exception. In Mine Action - Investigation Reports from the Royal Belgian
th Air Force; InTechOpen: London, UK, 2017; pp. 267-322.
15. Dori, a.
Introduction to Synthetic Aperture Sonar. In Proceedings of the 2019 IEEE Radar Conference (RadarConf), Boston, MA
, USA, 22-26 April 2019; pp. 1-90.
16. Atherton, M.
Echo Thiab Imaging, Sidescan, Thiab Encyclopedia of Scanning Sonar Operations; OysterInk Publishing: Vancouver,
BC, Canada, 2011; ISBN 098690340X.
17. Rao, C.; Mukherjee, K.; Gupta, S. (1999).
Raj, A. Phoha, S. Underwater mine detection using pattern analysis of
side-scan sonar images. In the Proceedings of the 2009 American Conference on Control, St. Louis, MO, USA, June 10-12, 2009; pp.

18. Dobek, GJ. In the Minutes of Oceans 2007 - Europe, Aberdeen, UK, 18-21 Lub Rau Hli 2007; pp. 1–6.
19. Reed, S.; Petilot, Y. Bell, J.
A method for automatic detection and extraction of signatures from side-scan sonar mines. IEEE J.
Oceans. project. 2003, 28, 90–105.

20. Klausner, N. Azimi-Sadjadi, M.R.; Tucker, J.
D. Identification of underwater targets from multi-platform sonar images using multi-channel coherence analysis
. Proceedings of the 2009 IEEE International Conference on Systems, Humans and Cybernetics, San Antonio

, Texas, USA, 11-14 October 2009; pp. 2728-2733.
21.
Ronner, F.; Knaul, C.; Jens, W. Ebert, A. Side-scan sonar image resolution and automatic object detection, classification and recognition
.
In Oceans '09 IEEE Bremen Proceedings: Balancing Technology and Future Needs, Bremen, Germany,
, 11-14 May 2009; 1-8.
22. Hożyń, S.; Zaewski, J.
Coastline Detection and Terrain Segmentation for Autonomous Surface Vehicle Navigation Siv
Optical System. Sensors 2020, 20, 2799. https://doi.org/10.3390/s20102799.
23. Hożyń, S.; Żak, B. Local Image Feature Matching or Real-Time Seabed Monitoring Applications. J.
Mart Engineering Technology. 2017, 16, 273–
282. https://doi.
org/10.1080/20464177.2017.1386266.
24.
A new multi-target side-scan sonar image segmentation algorithm.
Proceedings of the 2007 IEEE International Conference on Robotics and Bionics (ROBIO), Sanya, China, 15–18 December 2007
; pp. 2110-2114.
25. Om, H.
; Biswas, M. Improved Image Noise Reduction Method Based on Wavelet Threshold. J. The information process.
2012,
26.Hożyn
,S.;Żak,B.SegmentationAlgorithmUsingMethodofEdgeDetection.SolidStatePhenom.
2013, 196, 206–211. [CrossRef]
27. Celik, T.; Tjahjadi, T. A new segmentation method for side-scan sonar images.
IEEE J.Ocean. qhov project. 2011, 36, 186–194. [CrossRef]
28.
Wei, S. Liang, H. Myers, V. An automated adaptive sensing method for self-detection using side-scan sonar data. In Proceedings of the 2009 IEEE International Conference on Systems, People and Cybernetics
, San Antonio, TX, USA, 11-14 October 2009
; pp.
553-558: I.
29. Neumann, M.; Knaul, C.; Nolte, B.
; Brecht, D. Jens, W. Ebert, A. Object Detection of Man-Made Objects in Side Scan Sonar Images
Segmentation-Based False Positive Reduction. J. sound people. Yes. 2008, 123, 3949. [CrossRef]
30.

A robust and fast method for side-scan sonar image segmentation using non-native
despeckle and active contour models. IEEE range. sword. 2017, 47, 855–872. [Cross-Reference]
31.
Acosta, GG; Villar, S.A. A two-dimensional CA-CFAR technique for online object detection from side-scan sonar data.
IEEE J.
Oceans. qhov project. 2015, 40, 558–569. [Cross-Reference]
32.
Ye, X.-F.; Zhang, Z.-H. Liu, P.
X.; Kev, H.-L. Sonar Image Segmentation Based on GMRF and Level Light Model. Marine Engineering 2010,
37, 891–901. [Cross-Reference]
33. Fei, T.; Kraus, D. Dempster-Shafer Theory-Backed Expectation-Maximization Method and Its Application to Separation of Sonar Images
.
Nyob rau hauv 2012 Proceedings of the IEEE International Conference on Acoustics, Speech and Signal Processing (ICASSP),
Kyoto, Nyiv, 25-30 March 2012; pages 1161–1164. [Cross-References]
34. Szymak, P.; Piskul, P.
; Naus, K. Results of Pre-Trained Deep Learning Neural Networks for Object Classification in Underwater Videos
. Remote Sens. 2020, 12, 3020. [CrossRef]
35.
To hug.; Wu, Z. Li, J. Classification of underwater targets in side-scan sonar images using deep learning and semi-synthetic
datasets. IEEE Access 2020, 8, 47407–47418. [CrossRef]
36. Attaf, Y.; Boudra, A.O.; Ray, C. (1999).
Width Based Research Inspector on a Sidescan Sonar. Proceedings of the Ocean 2016-Shanghai, Shanghai, China, 10-13 April 2016. [CrossRef]
37. Wu, M.; Wang Qi
Rigar, E.; Li , K. Zhu , W. Nws , B. Yan , T .
ECNet: A Efficient Collaboration for Segmentation of Side-Scan Sonar Images
. Sensors 2019, 19, 2009. [CrossRef] [PubMed]
38. Abu, A.; Diamond, R.

A statistical method for detecting underwater objects in sonar images. IEEE Sens. J.2019,
19, 6858–6871. [CrossRef]
39.
McKay, J. Monga, V.; Raj, R.G. Rugged Sonar ATR for Sparse Classification with Bayesian Exposure Correction.
IEEE range. Ntiajteb Science.
Remote Sensing 2017, 55, 5563–5576. [CrossRef]
40.
Williams, DP Underwater object classification in synthetic aperture sonar dluab siv sib zog nqus convolutional neural networks.
Proceedings of the 2016 23rd International Conference on Pattern Recognition (ICPR), Cancun, Mexico, December 4–8, 2016;
p. 2497–2502.

41.Dobeck, GJ; Wellert, Dr. Real-time performance of the fusion algorithm for computer aided detection and mine classifications in the coastal environment.
Journal of Oceanography in 2003. Celebrating the Past. . .
Future-proof Collaboration (IEEE Catalog.
When. 03CH37492), San Diego, CA, USA, September 22-26, 2003; volume 2, p. 1119–1125: fig.
42. Saisan, P. (1999).
; Kadambe, S. Shape-normalized subspace analysis for mine detection. 2008 Proceedings of the 15th IEEE
International Image Processing Conference, San Diego, CA, USA, 12-15 October 2008; pages 1892–1895.
43.
Qingli, H.; Feng, S.L.; Chapple, P.B.
; Buzendum, A.; Reeds, CH; Tran, L.C.
Deep Gabor Neural Networks for Automatic Detection of Land-Like Objects
in Sonar Images. IEEE Access 2020, 8, 94126–94139. [Cross reference]

DrillBit

The Report is Generated by DrillBit Plagiarism Detection Software

Submission Information

Author Name	moin
Title	paper4
Paper/Submission ID	756521
Submission Date	2023-05-30 10:46:11
Total Pages	11
Document type	Research Paper

Result Information

Similarity **15 %**

Sources Type

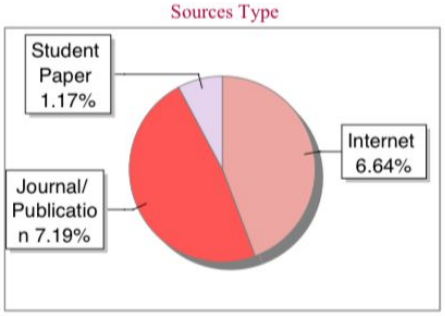

Report Content

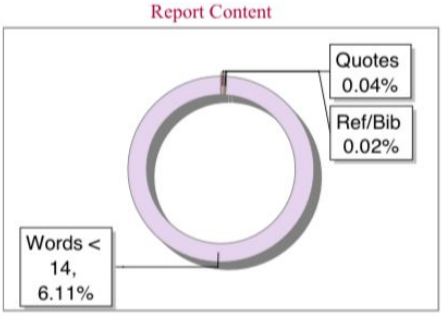

Exclude Information

Quotes	Not Excluded
References/Bibliography	Not Excluded
Sources: Less than 14 Words Similarity	Not Excluded
Excluded Source	**0 %**
Excluded Phrases	Not Excluded

A Unique QR Code use to View/Download/Share Pdf File

DrillBit

DrillBit Similarity Report

15	38	B
SIMILARITY %	MATCHED SOURCES	GRADE

A-Satisfactory (0-10%)
B-Upgrade (11-40%)
C-Poor (41-60%)
D-Unacceptable (61-100%)

LOCATION	MATCHED DOMAIN	%	SOURCE TYPE
1	www.mdpi.com	2	Internet Data
2	IMAGE CAPTIONING USING DEEP LEARNING TECHNIQUES BY 19031D6406 Yr-2021 SUBMITTED TO JNTU	1	Student Paper
3	A Hierarchical Learning Approach for Human Action Recognition by Lemieux-2020	1	Publication
4	www.mdpi.com	1	Internet Data
5	www.mdpi.com	1	Internet Data
6	downloads.bbc.co.uk	1	Publication
7	mdpi.com	1	Internet Data
8	www.dx.doi.org	1	Publication
9	medinform.jmir.org	<1	Publication
10	IEEE 2014 International Joint Conference on Neural Networks (IJCNN) by	<1	Publication
11	www.dx.doi.org	<1	Publication
12	arxiv.org	<1	Publication

13	Hybrid Ventilation System and Soft-Sensors for Maintaining Indoor Air Quality an by Vadamalraj-2020	<1	Publication
14	link.springer.com	<1	Internet Data
15	Road-map assisted ground moving target tracking by Marti-2006	<1	Publication
16	1library.co	<1	Internet Data
17	IEEE 2018 26th Telecommunications Forum (TELFOR)- Belgrade, Serbia, by Popovac, Milivoje - 2018	<1	Publication
18	mdpi.com	<1	Internet Data
19	www.atmos-chem-phys.net	<1	Publication
20	arxiv.org	<1	Internet Data
21	koreascience.or.kr	<1	Publication
22	IEEE 2014 IEEE 10th International Colloquium on Signal Processing by	<1	Publication
23	mdpi.com	<1	Internet Data
24	researchspace.ukzn.ac.za	<1	Publication
25	arxiv.org	<1	Publication
26	Depth Super-Resolution on RGB-D Video Sequences With Large Displaceme, by Wang, Yucheng Zhan- 2018	<1	Publication
27	vtechworks.lib.vt.edu	<1	Internet Data
28	IEEE 2009 American Control Conference - St Louis, MO, USA (20090610-200906 by Rao-2009	<1	Publication
29	Automated diagnosis of coronary artery disease (CAD) patients using op by Davar-217	<1	Publication

30	bcmj.org	<1	Internet Data
31	christpublicschoolmysore.org	<1	Internet Data
32	smw.ch	<1	Internet Data
33	Thesis Submitted to Shodhganga Repository	<1	Publication
34	www.frontiersin.org	<1	Publication
35	www.network.bepress.com	<1	Publication
36	coek.info	<1	Internet Data
37	moam.info	<1	Internet Data
38	Utilization of fatigue test to predict stripping of asphalt concrete m by AlKofahi-2019	<1	Publication